

Implications for CO₂ emissions and sinks changes in western China during 1995–2008 from atmospheric CO₂ at Waliguan

By F. ZHANG¹ and L. X. ZHOU^{2*}, ¹College of Global Change and Earth System Science, Beijing Normal University, Beijing, China; ²Chinese Academy of Meteorological Sciences (CAMS), China Meteorological Administration (CMA), Beijing, China

(Manuscript received 20 August 2012; in final form 19 December 2012)

ABSTRACT

Carbon dioxide (CO₂) emissions and sinks in western China are estimated and implied from atmospheric CO₂ measured at Waliguan during the period of 1995–2008. The observed CO₂ data are first classified as background, elevated, and sequestration, using a modified background identification method. Comparing it with two other methods tests the applicability of the method. By using this method, approximately $17.2\% \pm 1.2\%$ and $10.1\% \pm 0.8\%$ of all observed data are identified as elevated and sequestered CO₂, respectively, the percentages (occurrence rates) for both of which increased during 1995–2008. CO₂ emissions in western China have enhanced significantly in all seasons during the past 14 yr. Annual mean growth rates of CO₂ emissions in the region increased by $\sim 8.4 \text{ Tg C yr}^{-1}$ ($3.9\% \text{ yr}^{-1}$) during 1995–2008 but accelerated after 2000 to $\sim 12.6 \text{ Tg C yr}^{-1}$ ($6.2\% \text{ yr}^{-1}$). The growth rates of CO₂ emission in western China are lower than the rest of the country. The annual mean emissions in the country during 1995–1999 and 2000–2006 are thought to be approximately 5.5 and 6.5 times higher than in western China, respectively. However, the growth rates of CO₂ emissions in western China are higher than global increase rates as reported by other studies. CO₂ sinks in western China varied from $86.0 \text{ Tg C yr}^{-1}$ in early 1995–1999 to $106.2 \text{ Tg C yr}^{-1}$ in 2005–2008. The most prominent change occurs in summer, indicating enhanced sequestration of photosynthetic CO₂ taken up by vegetation. The growth rates in sequestered CO₂ cannot keep up with the increase of CO₂ emissions in the region. If this continues, it could potentially impact on the global carbon budget.

Keywords: carbon dioxide (CO₂), data selection, emissions and sinks, trends, western China

1. Introduction

Determining the impact of regional carbon dioxide (CO₂) exchanges on the global carbon budget is an essential step towards understanding and managing the budget. With rapid economic development, reported growth of CO₂ released from fossil fuel combustion and cement manufacturing over the 2001–2006 period has been dominant in developing countries, with 54% of the global increase in CO₂ emissions coming from China alone (Raupach et al., 2007). China has become the largest national source of CO₂ emissions during recent years (Gregg et al., 2008; Peters et al., 2012). On the basis of two publicly official energy data sets for China for 1997–2010, CO₂ emissions have

been calculated with a 1.4 Gt emission gap in 2010 between national and provincial statistics (Guan et al., 2012). Such an uncertainty of CO₂ emissions would result in an incorrect understanding and modelling of the global carbon cycle. Since 2000, China has implemented a national strategy to develop western regions and as a consequence, economic sectors that use petroleum have also been rapidly expanding. Therefore, a question arises of how CO₂ emissions over a regional as well as national scale change or are influenced under such a policy. In order to answer this question, there is a need to reduce the uncertainty in estimating regional and national emissions and to learn the extent to which the regional changes impact the global carbon budget.

The vegetation of Asia includes a broad range of temperate and boreal forests, grassland, and desert, and is perhaps one of the critical and sensitive regions in the global climate system. Several studies have reported that

*Corresponding author.
email: zhoulx@cams.cma.gov.cn

the carbon budget in China is primarily driven by land-use changes inferred by inventory and satellite data along with model simulations (e.g. Fang et al., 2001, 2004; Lal, 2004; Huang and Sun, 2006; Piao et al., 2007, 2009; Mu et al., 2008; Ren et al., 2011, 2012; Tian et al., 2011a, 2011b; Lu et al., 2012). Large-scale reforestation and afforestation programs conducted in western China since the 1980s have been studied as being a main cause of regional carbon sinks (Fang et al., 2001). Consequently, the balance of CO₂ budget in China is a large issue under the situation of high anthropogenic emissions and land use changes (Tian et al., 2011a).

Globally, CO₂ flux shows large discrepancies in different continents and regions (Sarmiento et al., 2010) with a significant imbalance in the global budget due to the lack of regional flux investigations (Turnbull et al., 2011), including uncertainties in anthropogenic emission estimates (Francey et al., 2010). The estimated trends of CO₂ emissions and sinks possess a high degree of uncertainty in different continental areas based on top-down and/or bottom-up methods (e.g. Francey et al., 1995; Fan et al., 1998; Bousquet et al., 1999, 2000; Pacala et al., 2001; Gurney et al., 2002; House et al., 2003; Maksyutov et al., 2003; Peylin et al., 2005; Ballantyne et al., 2012). To some extent, the uncertainties are confined to limited long-term observed data over regional scale.

Measurements of atmospheric CO₂ can reflect the information on the local/regional anthropogenic and natural perturbation. This uneven distribution of sources/sinks usually causes large spatial and temporal CO₂ variations (Tans et al., 1996). Fortunately, we can track the differences in fossil fuel carbon exchanges as well as the terrestrial CO₂ fluxes of different regions. In China, the longest observational record of atmospheric CO₂ has been obtained from remote Waliguan since the 1990s (Zhou et al., 2003). Based on these data obtained in earlier years, the seasonality, secular trend, annual cycle, and inter-annual variability of atmospheric CO₂ have been presented and characterized (Zhou et al., 2003, 2005, 2006). For example, Zhou et al. (2003) discussed the background characteristics after filtering the episodes by using a meteorology method. Afterwards, a few field campaigns or research experiments at various remote and urban sites in China were conducted in the past few decades (e.g. Wang et al., 2002; Zhang et al., 2008; Liu et al., 2009; Wang et al., 2010). Most of these studies mainly focused on the levels, seasonality and spatial variation at urban or suburban sites. In this study, we will estimate and imply changes of CO₂ emissions and sinks in western China from the episodes of atmospheric CO₂ measured at Waliguan over 1995–2008. The primary objective is to provide a basic understanding of regional/local impacts on the changes of CO₂ emissions and sinks under the situation of high anthropogenic emissions and

land use changes in western China. The observed data are first classified as background, elevated, and sequestered CO₂ using a modified background identification method. Comparing it with other methods tested the applicability of the method. CO₂ emissions and sinks are estimated from the selected elevated and sequestered CO₂ episodes. Finally, the changes of CO₂ emissions and sinks in western China are inferred.

2. Data and methods

2.1. Data

The CO₂ data are from the long-term continuous retrievals of atmospheric CO₂ mixing ratios by a Licor6251 non-dispersive infrared NDIR analyzer at Waliguan (36.28N, 100.90E, 3816 m a.s.l.) since November 1994. Both CO₂ regional sources and sinks information observed at Waliguan represent a relatively large-scale area due to the high altitude and extensive topography within the region. Therefore, measurements from the site can provide essential information on sources and sinks within the Eurasian continent (Zhou et al., 2005, 2006). A detailed discussion of the site, measurements, and calibrations for the system has been addressed in previous studies (Wen et al., 1997; Zhou et al., 2003). The data have also been updated and reported on the WMO X2007 scale (http://ds.data.jma.go.jp/gmd/wdcgg/products/summary/sum34/43_calibration.pdf). The data retrieval period in this study is 1995–2008. The overall CO₂ time series had data gaps from June 1997 to November 1998 due to reconstruction of the Waliguan main building. In addition, some data was missing in the winter of 2001 and invalidated during June 2006–February 2007 which was due to calibration and instrumental malfunction (e.g. leakage of the inlet line connected to cryo-coolers).

2.2. Data selection

2.2.1. Data selection method. A remote location regarded as having no local or regional source/sink influences is usually selected for measuring background conditions. However, within the planetary boundary layer (PBL), a ground-based station like Waliguan is exposed to a wide variety of situations, including air, which is locally or regionally influenced. The observed episodes of anomalous signals presented in the time series could reflect changes of regional emissions and sinks. The objective of selecting the data is to identify those hourly CO₂ values that are representative of well-mixed air at the latitude of Waliguan as well as those of which that are affected by some known local/regional phenomenon.

Using an appropriate filter method to distinguish the different conditions is the first step. Data selection can be based on independently measured parameters, such as wind speed and direction, or by using a statistical approach for rejecting certain data, or combined meteorological and statistical filters. The basic assumption is that the concentration of CO₂ in well-mixed air should change by only a small amount over several hours at extremely remote monitoring sites, such as the South Pole, Antarctica, where the hour-to-hour variability is very small (<0.1 ppm, Gillette et al., 1987).

Thoning et al. (1989) also used this assumption to identify CO₂ background conditions at Mauna Loa, but because Mauna Loa is not as remote as the south pole, they used a larger criteria for the initial selection process: instability of the CO₂ concentration >0.2 ppm within 1 hour and changes in the CO₂ concentration >0.25 ppm from 1 hour to the next were rejected. Any effects from volcanic episodes in the diurnal variation that typically occurred (11:00–19:00 LT) were temporarily removed. Finally, they applied an iterative statistical approach of a smooth spline curve to weighted daily averaged CO₂ values, and flagged hourly data greater than two standard deviations from the daily average.

This method assumes that the background signal varies very slowly relative to contributions of the regional signal; these assumptions are suitable to Waliguan where the variation of the baseline signal is in the order of weeks while the regional signal varies from hourly to daily. Thus, we also apply the Thoning method to Waliguan data, without the step of removing diurnal cycle influence due to no existing volcanic episodes as well as insignificant terrestrial biospheric fluxes around the site. By using the Thoning method, approximately 40% of all observed CO₂ data are selected as background data. However, according to Zhou et al. (2003), they obtained almost 70% of all the background data by using meteorology as a filter. Therefore, we make modifications based on the Thoning method.

The Licor6251 NDIR system is similar to the instrument at Mauna Loa and is used to measure CO₂ at Waliguan. The measurement errors are expected to be random and the overall measurement precision for the instrument is less than 0.1 ppm as determined from the standard deviation of repeated measurements of an approximately 365 ppm standard gas (Zhou et al., 2003). The variability within an hour test is also applied – if CO₂ hourly means with standard deviations >0.3 ppm are initially removed to distinguish the visible instrument fluctuation. Similar to the Thoning method, changes in the CO₂ concentration >0.3 ppm from one hour to the next were rejected.

Waliguan is located at the edge of the northeastern part of the Tibetan Plateau (high altitude). The area surrounding the site is pristine, with sparse vegetation consisting

mostly of arid and semiarid grassland and the diurnal variation is relatively small (Zhou et al., 2003). Large variabilities are usually observed at Waliguan due to external polluted air parcels undergoing long distance air transportation during short time periods (e.g. 3–5 d). This causes either an increase or decrease of CO₂ concentrations that can last anywhere from hours to several days.

Consequently, although the differences in the two consecutive hourly values are insignificant (<0.3 ppm) during the periods, they are actually non-background values. If they are not rejected at this step, they would affect the curve fit. In order to alleviate these problems, our method for this final selection was to temporarily remove 30% of the data, which are statistically calculated as maximum or minimum values by evaluating two weeks of hourly data at a time. A two-week work window is chosen because the data observed during this short period could potentially include both polluted/sequestered episodes and baseline information, but not be influenced by long-term trends or seasonality. The remaining data over the two weeks are then smoothed using an approach of moving an average curve fit where the first hourly concentration of the two weeks, which differed from the average of the curve by more than twice the standard deviation (σ) of the two weeks, were flagged as a non-background value. This is identified as pollution or sequestration according to whether or not this value is larger than the average of the curve. The process then moves to test the second hourly value in another 2-week period. At this point, those values with changes >0.3 ppm in two consecutive hourly concentrations and 30% hourly values previously removed at the beginning of the selection were added if they are now within 2σ of the spline. Daily, monthly and annual means are calculated from the final selected data.

The time series of CO₂ identified by our modified method is shown in Fig. 1. More than 70% of all observed CO₂ has been selected as background data. Elevated CO₂ mixing ratios represent contaminations from local or regional emissions/sources. They were observed with some episodes (red dots) distributed above the background levels (black dots). Back-trajectories for the specific periods of high CO₂ have correlated these polluted episodes to regions with large emission sources (Zhang et al., 2011) that are especially active in the winter/early spring season. CO₂ with relatively low values correspond to sequestrations primarily due to enhanced photosynthetic effects (green dots).

2.2.2. Applicability of the method. To examine the applicability of our modified method for the identification of CO₂ background conditions, overall long-term changes of CO₂ monthly means identified by the Thoning method

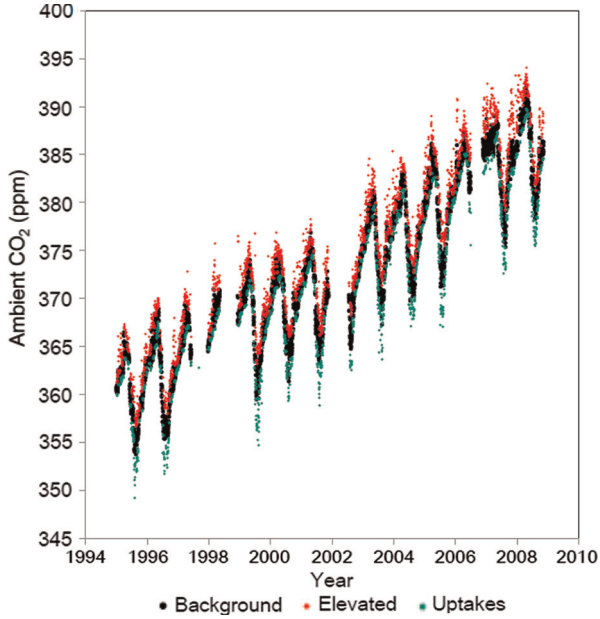


Fig. 1. Time series of CO₂ measurements between 1995 and 2008 at Waliguan identified by our modified data selection method.

and our modified method at Waliguan during 1995–2008 are shown in Fig. 2. The monthly means obtained from the Thoning method and our modified approach

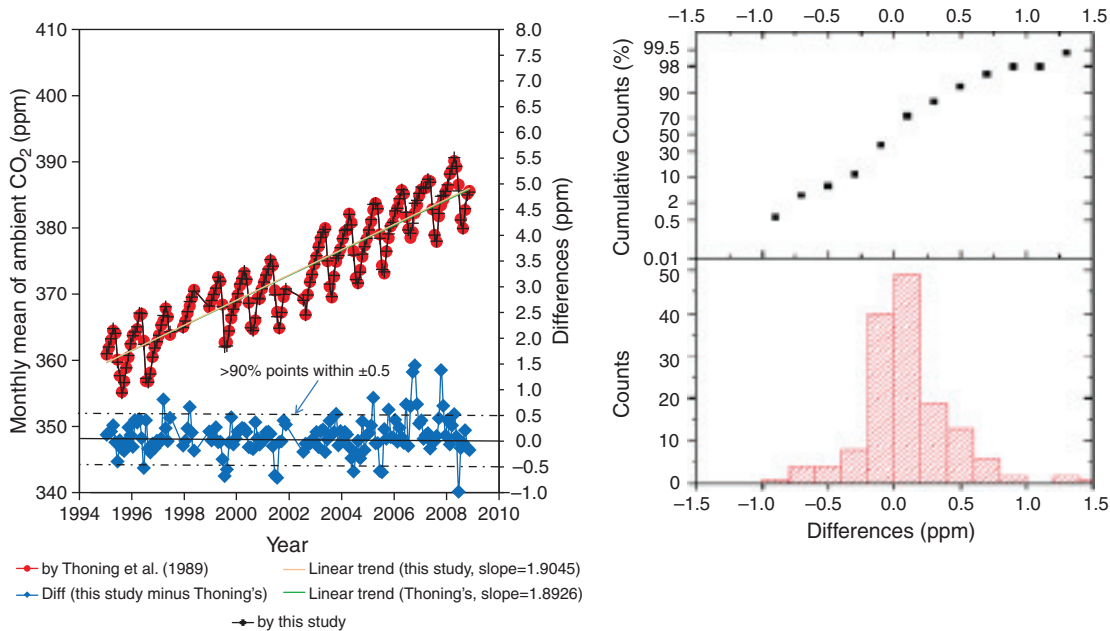


Fig. 2. Overall long-term changes of CO₂ monthly means from continuous measurements identified by Thoning et al. (2003) (red dots) and by this study (black crosses) at Waliguan during 1995–2008, and the linear trends of the monthly means for the two methods are very similar with slopes of 1.9045 and 1.8926, respectively. The differences between the Thoning method and our method (blue dots) are also shown on the left y-axis. A histogram and probability of the differences, which showed more than 90% of all points are within ± 0.5 ppm, are embedded in the top and left panel of the figure.

are without significant differences, with more than 90% of all points within ± 0.5 ppm, 85% points within ± 0.25 ppm and about 70% points closer to zero from the CDF and histogram of the differences embedded in the top and left panel of Fig. 2. The linear trends of the monthly means for the methods are very similar with slopes of 1.9045 and 1.8926 by our method as well as the Thoning method.

To further investigate how different selection methods can affect the CO₂ seasonality over long-term periods, we compared the results identified by using the method of Thoning et al. (1989) and Zhou et al. (2003) with this study (Fig. 3). Zhou et al. (2003) applied a combined statistical and meteorological parameter as a filter to select CO₂ data at Waliguan. However, their method removes the hourly CO₂ values associated with the wind direction from polluted wind sectors (e.g. air masses from northeastern and north in summer) as well as CO₂ hourly values during calm conditions, during periods with horizontal wind speed > 10 m/s, or vertical wind speed $> \pm 1$ m/s. Finally, they used an iterative approach by a fitting curve (weighted least squares) for each day using criteria involving the differences for each remaining hourly points and curve $> 3\sigma$ to further smooth the data.

In Fig. 3, the overall characteristic of the CO₂ seasonal cycle identified by the three methods did not exhibit a large

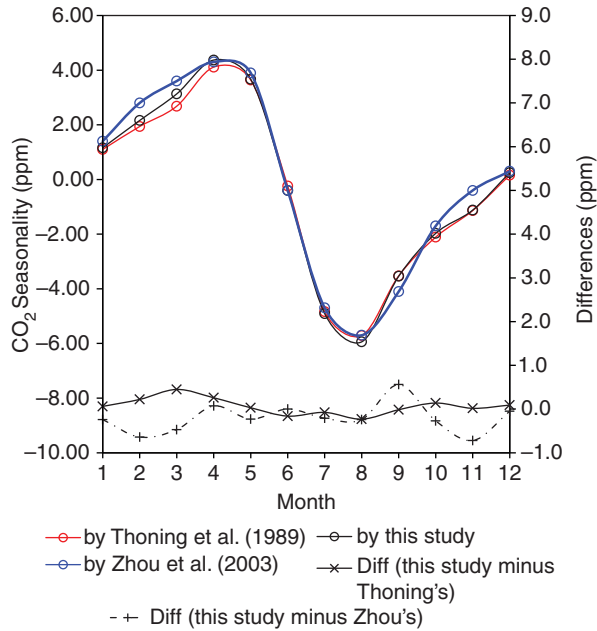


Fig. 3. Mean CO₂ seasonality identified by Thoning et al. (2003) (red circle), Zhou et al. 2003 (blue circle) and this study (black circle) during 1994–2000. The differences of seasonal trends between the method by the other’s method and our method are also plotted below.

difference in that the CO₂ seasonality showed an early spring (in April) maximum and late summer (in August) minimum. The differences between our modified method and the Thoning method are almost close to zero in all months whereas the discrepancy between our method and the Zhou method is more apparent. The largest differences always appear in cold months, such as February or March,

where the CO₂ concentrations calculated by the Zhou method are approximately 0.5–0.8 ppm higher than our modified method. CO₂ concentrations in these months obtained by the Thoning method are only slightly lower than that identified by our method. However, all three methods observed seasonal amplitudes of 10 ppm. Table 1 lists the annual means of CO₂ calculated from the hourly values as identified by the three methods.

The differences in the annual means between the Thoning method and our modified approach changed from approximately -0.1 ppm to 0.1 ppm over the period of 1995–2008 while the discrepancies with Zhou’s method are also within ± 0.1 ppm. This small bias indicates that our modified method is ideal, not only because it is resistant to year-to-year and seasonal variations of ambient CO₂ during long-term periods, but also due to more data being retained for the background conditions. In addition, the modified method is more efficient compared to Zhou et al. (2003) for which they also needed to take into account more meteorological conditions. Consequently, elevated CO₂ due to regional/local emissions and sequestered CO₂ caused by photosynthesis could be selected from all the observed time series.

3. Results and discussion

3.1. Selected data analysis

3.1.1. Percentages of selected CO₂ data. Table 2 lists percentages for selected background, elevated and sequestered CO₂ data in each year by using our method. A percentage of $72.8\% \pm 1.4\%$ of all observed CO₂ data have

Table 1. Annual means of CO₂ calculated from the hourly data identified by the three methods

Year	CO ₂ annual mean, in ppm				Differences, in ppm		
	by Thoning et al. (1989)	s.d.	by Zhou et al. (2003)	This study	s.d.	Diff (this study-Thoning’s)	Diff (this study-Zhou’s)
1995	360.48	2.9	360.6	360.51	3.0	0.03	-0.09
1996	362.18	3.5	362.2	362.22	3.6	0.04	0.02
1997							
1998							
1999	367.93	3.3	367.9	367.86	3.5	-0.07	-0.04
2000	369.37	2.8	369.5	369.46	2.9	0.09	-0.04
2001	370.68	3.2		370.65	3.4	-0.03	
2002							
2003	375.51	3.2		375.65	3.1	0.14	
2004	377.16	3.3		377.08	3.3	-0.08	
2005	379.35	3.3		379.44	3.5	0.09	
2006							
2007	384.07	3.0		384.14	3.1	0.07	
2008	385.78	3.3		385.78	3.4	0.00	

Table 2. Percentage for background, polluted and sequestered CO₂ data in each year

Year	1995 (%)	1996 (%)	1997* (%)	1998* (%)	1999 (%)	2000 (%)	2001 (%)	2002* (%)	2003 (%)	2004 (%)	2005 (%)	2006* (%)	2007 (%)	2008 (%)
Background	74.7	73.5			72.2	74.9	72.3		72.8	73.6	71.1		70.9	71.9
Polluted	15.9	15.9			17.7	15.4	17.8		18.5	16.1	17.2		18.6	18.4
Sequestered	9.4	10.6			10.1	9.7	9.9		8.8	10.3	11.7		10.5	9.7

*Percentages in the years not available are due to the data gaps caused by the instrument malfunction or calibrations during the measurement periods.

been selected as background data over the past 14 years while large CO₂ mixing ratios account for $17.2\% \pm 1.2\%$ of all data representing the contaminations influenced by local or regional emissions/sources from fossil fuel or biosphere sources. Relatively low values of CO₂ concentrations correspond to sequestered CO₂ suggesting photosynthetic activity (lower average percentage of $10.1\% \pm 0.8\%$). The percentages of background, elevated and sequestered data in different years reflect the changes in regional sources and sinks for CO₂ as well as the changes in meteorological conditions at Waliguan.

Figure 4 displays trends in the percentages for background, elevated and sequestered CO₂ data. It should be noted that the percentage of elevated data increased slightly from 15 to 16% during the 1995–2000 period and from 17 to 18% during the 2004–2008 period. This is likely a result of increased CO₂ sources and enhanced regional impacts in recent years. Such an increase is driven by anthropogenic emissions or natural releases, and thus cannot be sorted out

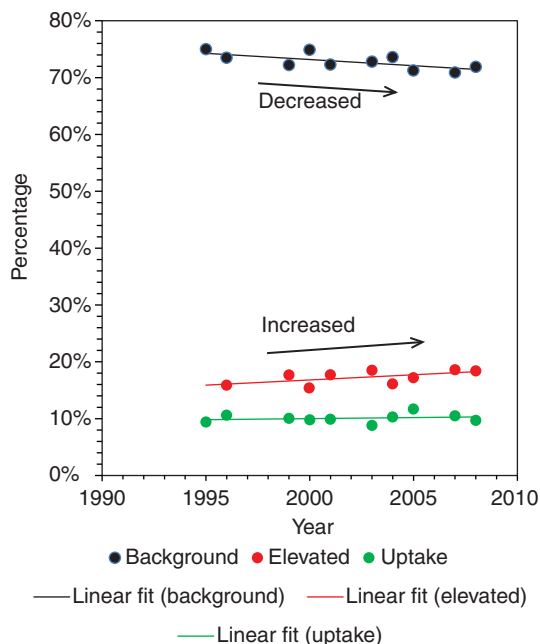


Fig. 4. Trends of the percentages for background, elevated, and sequestered CO₂ data.

due to all the information being included in the observations. The percentages of CO₂ data representing ‘sequestration’ also slightly increased from approximately 10 to 10.6% between 1995 and 2008 suggesting an increased trend of the occurrence of sequestered CO₂ in recent years in western China.

3.1.2. Time series of elevated and sequestered CO₂. We take elevated and sequestered CO₂ as an index in this study in order to investigate the long-term variations of CO₂ emissions and sinks. Daily averages are used to calculate the changes of CO₂ based on their corresponding background values. By convention, the CO₂ sink is reported as negative (removing CO₂ from the atmosphere) and its source as positive (adding CO₂ to the atmosphere). In this study, $\Delta\text{CO}_2(\text{E})$ refers to the amounts of emissions (typically positive values) and $\Delta\text{CO}_2(\text{S})$ reflects the magnitudes of sinks with negative values. They are calculated by using daily elevated and sequestered CO₂ minus background values, respectively. If $\Delta\text{CO}_2(\text{E})$ is more positive or $\Delta\text{CO}_2(\text{S})$ is more negative, that would reflect stronger CO₂ emissions or sinks.

Figure 5 shows the time series of elevated and sequestered CO₂ as indicated by $\Delta\text{CO}_2(\text{E})$ and $\Delta\text{CO}_2(\text{S})$ during 1995–2008. Significant fluctuations in $\Delta\text{CO}_2(\text{E})$ are exhibited which vary from 0 to approximately 5 ppm during the observed period. There is no apparent seasonal cycle indicated by $\Delta\text{CO}_2(\text{E})$, but $\Delta\text{CO}_2(\text{S})$ does display a significant seasonal variation with values of near zero in winter and negative in the summer (~ -5 ppm). The seasonality for $\Delta\text{CO}_2(\text{S})$ should be mainly attributed to enhanced photosynthetic sequestration in the summer which can lead to a sharp decline in atmospheric CO₂ mixing ratios in the northern hemisphere (Tans et al., 1990).

3.2. Implications of CO₂ emissions and sinks

3.2.1. Study area definition and estimates method. Analysis of air mass back-trajectories combined with long-term ambient air measurements can be used for ana-

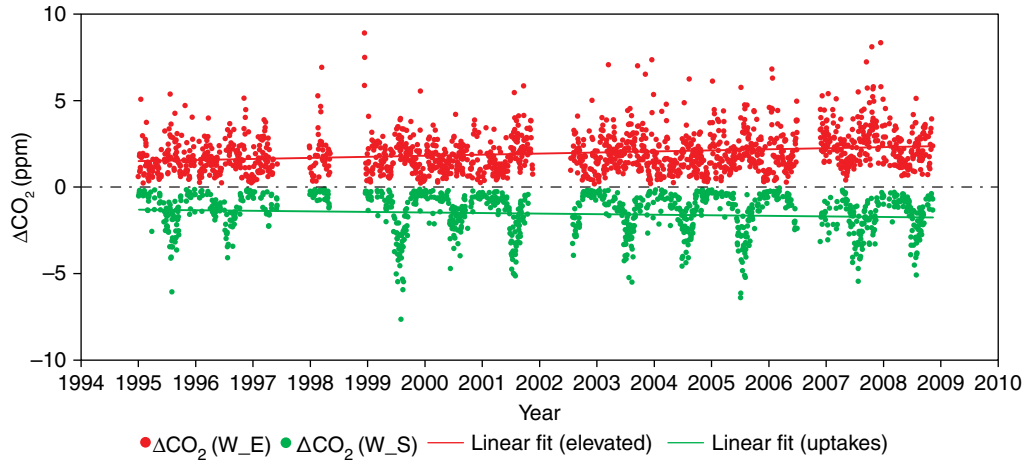


Fig. 5. Time series of elevated and sequestered CO₂ during 1995–2008.

lysing large-scale air pollutant transport and source identification at a receptor site (Stohl, 1996; Rousseau et al., 2004). Usually, the influence of air transport over a site

within 3–5 d is regarded as a regional impact. Therefore, in this study, we calculated five day (120 h) back-trajectories originating at 00:00, 06:00, 12:00 and 18:00 UTC by the

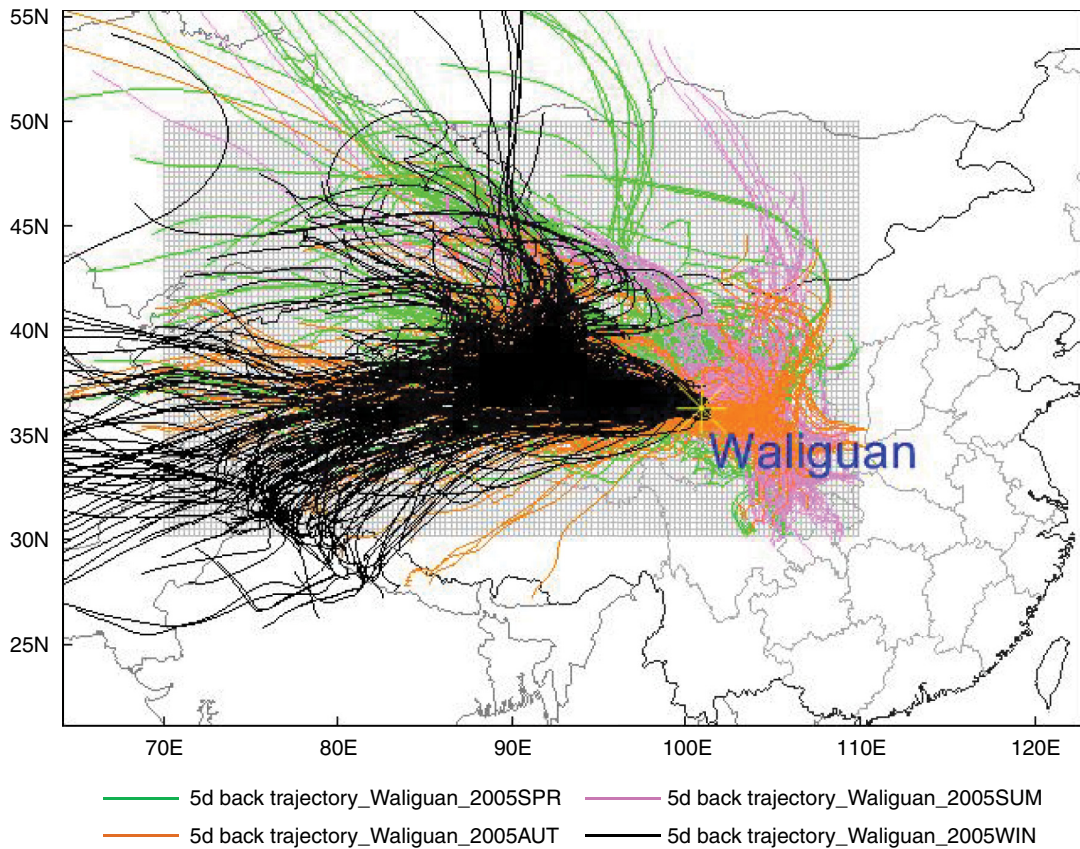


Fig. 6. Five-day (120 h) back-trajectories at Waliguan in 2005. The different colours indicate trajectory in different seasons. The back-trajectories originating at 00:00, 06:00, 12:00 and 18:00 UTC were calculated by the Hybrid Single-Particle Lagrangian Integrated Trajectory model (HYSPPLIT) (Draxler and Hess, 1998) using NCEP (National Centers for Environmental Prediction) reanalysis data. The arrival height of the trajectories was 500 m above ground level. A grid area, covered by almost trajectories of the whole year with latitude of 30°N–50°N and longitude of 70°E–110°E, has been identified, as include most of the region of western China.

Hybrid Single-Particle Lagrangian Integrated Trajectory model (HYSPLIT) (Draxler and Hess, 1998) using NCEP (National Centers for Environmental Prediction) reanalysis data.

The arrival height of the trajectories was 500 m above ground level, which has been shown to be the most representative for air sampled at Waliguan (Zhou et al., 2003). According to the paths and regions that the trajectories passed through, we have identified a grid area with latitude of 30N–50N and longitude of 70E–110E (Fig. 6). In this study, the estimated changes of CO₂ emissions could thus represent the specified grid area that covers most regions of western China.

Because the occurrences of elevated and sequestered CO₂ shows large variances over different periods, using $\Delta\text{CO}_2(\text{E})$ or $\Delta\text{CO}_2(\text{S})$ alone cannot provide a real and integrative estimate of sources and sinks. For example, in winter, high-sequestered CO₂ concentrations can be observed at any time but the frequency of occurrence (percentage of sequestered data) is usually low. Therefore, a weighted ΔCO_2 , which we define as $\Delta\text{CO}_2(\text{W_E})$ and $\Delta\text{CO}_2(\text{W_S})$, are calculated using $\Delta\text{CO}_2(\text{E})$ and $\Delta\text{CO}_2(\text{S})$ multiplied by their frequency of occurrence. We then estimate the amount of emissions and sinks using $\Delta\text{CO}_2(\text{W_E})$ and $\Delta\text{CO}_2(\text{W_S})$ multiplied by a conversion factor of γ ($\gamma = 36.7 \text{ Tg C/ppm}$). The conversion factor is calculated from atmospheric CO₂ reported as the dry air molar mixing ratio in ppm units (Sarmiento et al., 2010), which is then converted to Tg C of CO₂ in the atmosphere using the following relationships:

$$\begin{aligned} N_{\text{air}} &= \frac{m_{\text{atm}}}{\mu_{\text{air}}} \\ \mu_{\text{air}} &= 0.0289644 + 0.012011 \cdot (\chi_{\text{CO}_2} - 0.0004) \\ N_{\text{CO}_2} &= \chi_{\text{CO}_2} \cdot N_{\text{air}} \\ m_{\text{CO}_2} &= \mu_{\text{C}} \cdot N_{\text{CO}_2} \end{aligned}$$

where N_{air} is the number of moles in the atmosphere, m_{atm} is the dry mass of the atmosphere of the area covered by trajectories of the whole year with latitude of 30°N–50°N and longitude of 70°E–110°E (Fig. 6), which accounts for nearly 1.7253% of the total global surface area. In this case, the total dry mass of the atmosphere ($5.1352 \pm 0.0003 \times 10^{18} \text{ kg}$) estimated by Trenberth and Smith (2005) is multiplied by 1.7253% to obtain the m_{atm} . The molar mass of air (μ_{air}) in kg mol^{-1} for which we use the relationship given by Khélifa et al. (2007), ΔCO_2 is the dry air molar mixing ratio of CO₂ obtained by measurements, and $\mu_{\text{C}} = 12 \text{ g mol}^{-1}$ is the molar mass of carbon. The conversion factor we obtain is 36.70669 Tg C per ppm of dry air in January of 1995, decreasing to 36.70632 by

November of 2008. Thus, we use a conversion factor of 36.7 Tg C per ppm of dry air.

3.2.2. Seasonal changes of CO₂ emissions. Figure 7 illustrates the CO₂ emission changes derived from the weighted amounts of elevated CO₂ in different seasons between 1995 and 2008 in western China. CO₂ emissions as indicated by $\Delta\text{CO}_2(\text{W_E})$ increased significantly in each season during the past 14 yr. The upward trends in spring and summer are similar, with growth rates of approximately 1.2–1.3 Tg C yr⁻¹. However, $\Delta\text{CO}_2(\text{W_E})$ showed much larger year-to-year fluctuations during the spring with a low correlation coefficient value while during the summer exhibiting slight inter-annual changes with a smooth increasing linear trend. In autumn, $\Delta\text{CO}_2(\text{W_E})$ showed a rapid growth rate of $\sim 1.7 \text{ Tg C yr}^{-1}$ over the period of 1995–2008, with large year-to-year fluctuations. In winter, $\Delta\text{CO}_2(\text{W_E})$ showed the fastest upward trend and increased by approximately 4.0 Tg C yr⁻¹. The inter-annual variation in winter is also small and similar to that obtained in summer. The different growth rates of $\Delta\text{CO}_2(\text{W_E})$ observed during different seasons reflect the distinct seasonal characteristics of CO₂ sources in western China. The large inter-annual variations of $\Delta\text{CO}_2(\text{W_E})$ in spring and autumn indicated that these regional or local CO₂ sources (e.g. fossil fuel, biomass burning or respirations) changed significantly both in magnitude and type from year to year. In other words, the slight year-to-year fluctuations of $\Delta\text{CO}_2(\text{W_E})$ implied relatively constant CO₂ sources in the winter and summer seasons.

Overall, $\Delta\text{CO}_2(\text{W_E})$ increases much more dramatically in winter than in summer. According to our previous studies (Zhou et al., 2003; Zhang et al., 2011), CO₂ spikes in winter were closely associated with dominant air parcels especially from the northwestern regions of the site, such as the Taklimakan Desert and Tarim Basin, both of which have been largely developed in past decades due to a wealth of oil and gas resources. In summer, these spikes frequently occur due to prevailing air masses originating from north-eastern or eastern regions (e.g. Gansu and Shaanxi provinces).

Furthermore, we assert that anthropogenic CO₂ emissions west of the site change faster than eastern areas during previous decades. Surprisingly, we find that potential source regions of CO₂ are extensively distributed west of the site (Zhang et al., 2011), which was unexpected since the area is typically regarded as relatively remote and clean. High CO₂ concentrations in the area have also been retrieved based on the satellite data (Bai et al., 2010), which further indicates strong CO₂ sources. This change may be the result of emerging economies in western China during

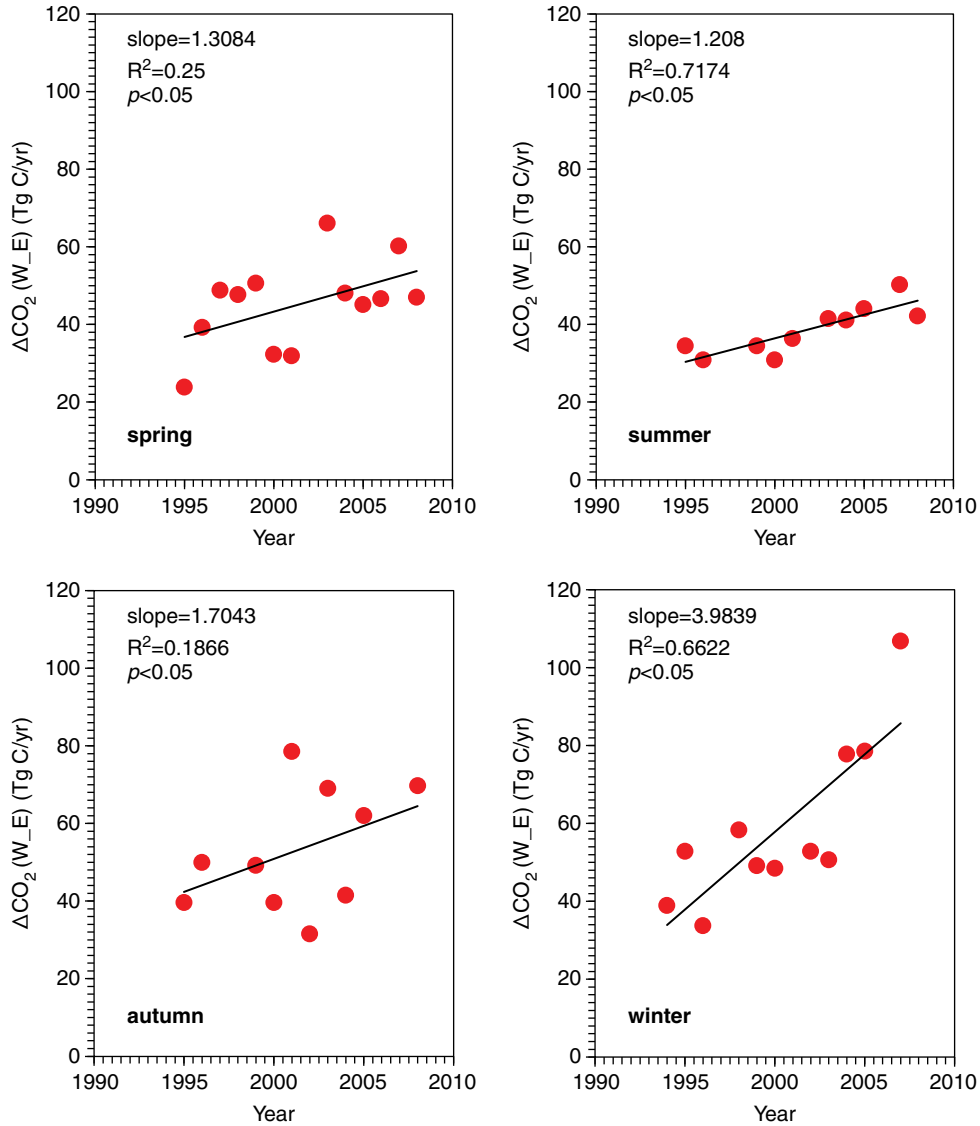


Fig. 7. CO₂ emission changes estimated from the weighted amounts of elevated CO₂ in different seasons between 1995 and 2008 in western China.

the past two decades thus leading to significant increases in CO₂ emissions.

The increasing ΔCO₂ (W_E) trend observed in autumn is stronger than in the spring. This suggests enhanced respirations due to autumn warming under climate change and growing atmospheric CO₂ concentrations according to Piao et al. (2008). They found that both plant photosynthesis and respiration increase during autumn warming, but the increase in respiration is greater by using process-based terrestrial biosphere model and satellite vegetation greenness index observations. Their simulations and observations indicated that northern terrestrial ecosystems may currently lose CO₂ in response to autumn warming from using historic climate data during the 1980–2002 period

(Piao et al., 2008). However, further studies are needed to demonstrate our observed enhanced increasing CO₂ emission trend in autumn.

3.2.3. *Seasonal changes of CO₂ sinks.* Figure 8 displays changes of the CO₂ sink derived from weighted amounts of sequestered CO₂ in different seasons between 1995 and 2008. The ΔCO₂ (W_S) values for every season except summer did not show significant upward or downward trends. The plain lines reflect CO₂ sinks due to the terrestrial ecosystem in western China and are relatively constant in the spring, autumn and winter seasons during the 1995–2008 period. The absolute value of

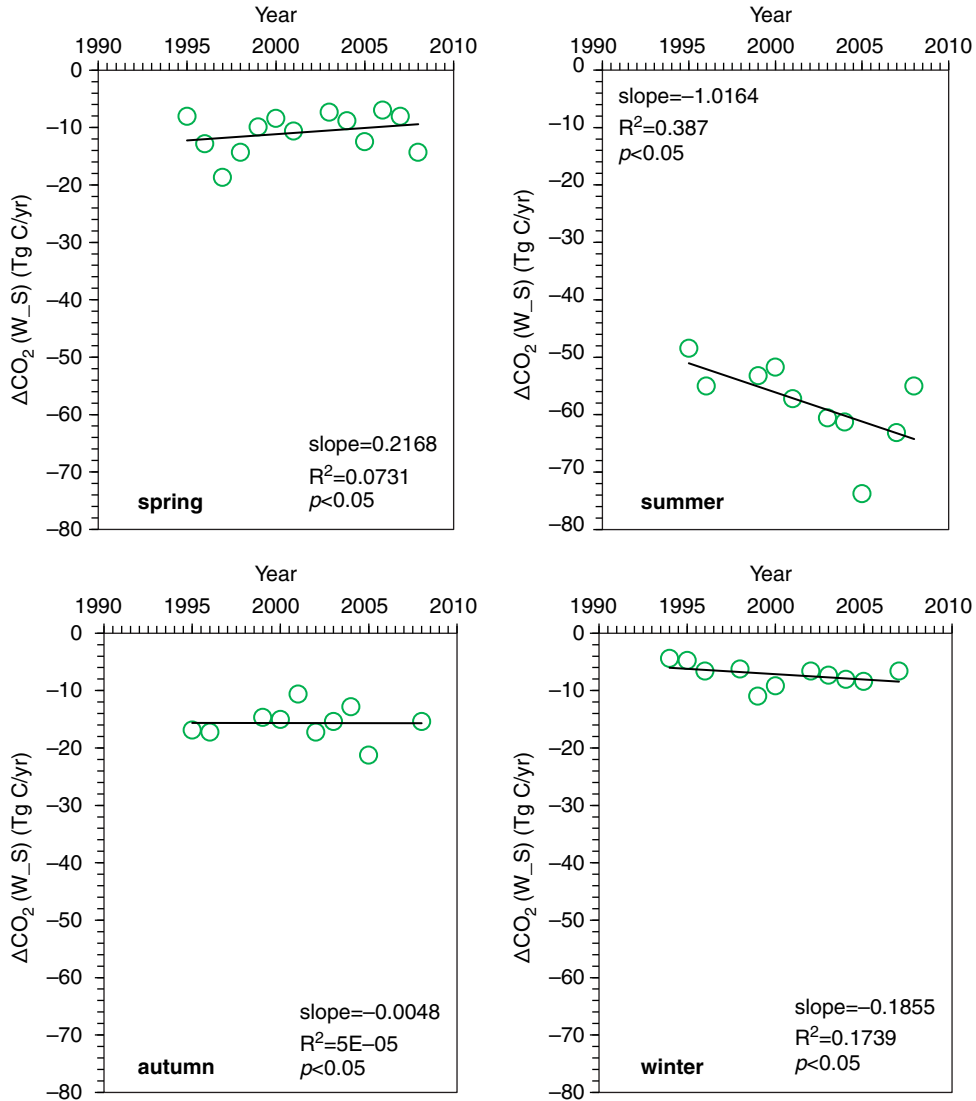


Fig. 8. CO₂ sink changes estimated from the weighted amounts of sequestered CO₂ in different seasons between 1995 and 2008 in western China.

ΔCO_2 (W_S) in winter is lowest ($< 10 \text{ Tg C yr}^{-1}$), indicating weak CO₂ sinks caused by decreased vegetation activity in the northern hemisphere mid-latitude during cold periods.

In the summer, the absolute values of ΔCO_2 (W_S) are larger (approximately $50\text{--}60 \text{ Tg C yr}^{-1}$) due to strong biosphere CO₂ sequestration by terrestrial ecosystems. The decreasing trend of ΔCO_2 (W_S) in summer implies a slight increase of CO₂ sinks with a growth rate of 1.0 Tg C yr^{-1} from 1995 to 2008. The increase may imply an enhanced terrestrial sink in western China driven by changes of several integral global change factors including solar radiation, precipitation, and vegetation fractional cover (Tian et al., 2011a).

3.2.4. Trends of CO₂ emissions. Figure 9 shows total annual emissions and sinks of CO₂ as indicated by ΔCO_2 (W_E) and ΔCO_2 (W_S) in each individual year from 1995 to 2008. Annual emissions of CO₂ exhibited a significant increasing trend with a yearly growth rate of approximately 8.4 Tg C yr^{-1} ($3.9\% \text{ yr}^{-1}$) during 1995–2008 which accelerated to $12.6 \text{ Tg C yr}^{-1}$ ($6.2\% \text{ yr}^{-1}$) during 2000–2008. This is most likely due to China implementing a national strategy in 2000 to develop western regions. Economic sectors that use petroleum have also rapidly expanded since 2000. By comparing the total emission growth rate of China, we estimated an increase in CO₂ emissions of 58% from 2000 to 2006, which is lower than the near 80% increase (at 10% annual growth) from all

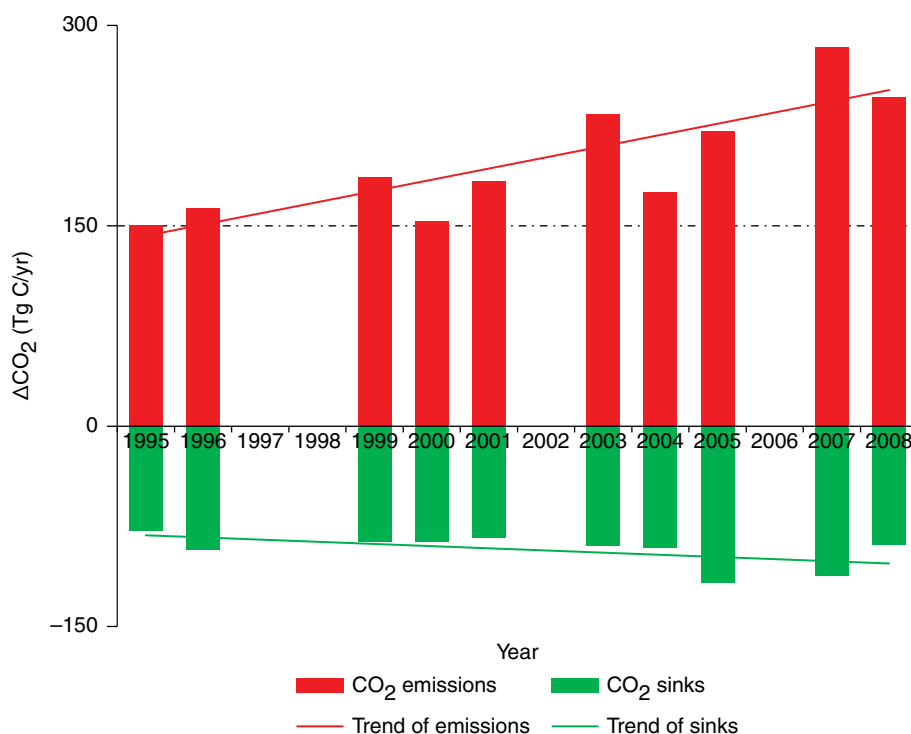


Fig. 9. Trend of CO₂ emissions and sinks estimated from the observed elevated and sequestered CO₂ during 1995–2008 in western China.

China during the same periods reported by Gregg et al. (2008).

The annual mean emissions changed from 167 Tg C yr⁻¹ in 1995–1999 to 193 Tg C yr⁻¹ during 2000–2006. Gregg et al. (2008) estimated that the country emitted 132 Tg C month⁻¹ in November 2005 and 142 Tg C month⁻¹ in September of 2006. One can thus roughly estimate an annual emission of 1644 Tg C in 2006 by using the average of monthly emissions in November 2005 and September 2006 multiplied by 12. According to the 10% annual growth during 2000–2006, one can also calculate the annual national emissions of nearly 926 Tg C in 2000 and 1256 Tg C during the 2000–2006 period. Consequently, the annual emission during 2000–2006 in the country is almost 6.5 times higher than that in western China. Additionally, we suppose the national annual emission in 2000 should be slightly higher or similar to that during 1995–1999, and thus the annual mean emission during the early years of 1995–1999 in the country is approximately 5.5 times higher than that in western China. The large discrepancy of CO₂ emission between western and eastern China has also been indicated by a short-term observed dataset from Shangdianzi, which is located in populated North China Plain (Turnbull et al., 2011). Based on the above assumption, the emission gap of CO₂ between western China and the rest of the nation has grown since 2000. However, due to the sharp acceleration of emission rates in western China, we imply

the numbers would be closer, and the emission gap between the western areas and other regions of China would be reduced with the rapid economic development over the country in the near future.

As compared to global emissions, the growth rates of CO₂ emissions in western China are much higher. For example, Le Quere et al. (2009) reported global CO₂ emissions from fossil fuel combustion, including small contributions from cement production and gas flaring, increased at a rate of 1.0% yr⁻¹ in the 1990s and 3.4% yr⁻¹ between 2000 and 2008. Canadell et al. (2007) also reported CO₂ emissions from fossil fuel burning and industrial processes increased with a similar growth rate of 1.3% yr⁻¹ for 1990–1999 to 3.3% yr⁻¹ for 2000–2006. The quickening trend of CO₂ emissions in western China since 2000 implied from changes of atmospheric CO₂ by this study is consistent with the trend globally. However, the reported anthropogenic CO₂ emissions by the above-mentioned studies are all sourced from CO₂ Information Analysis Center (CDIAC) compilations of reported national emissions based on slightly varying inventory methods. While our study just implies regional atmospheric changes in western China, which could provide an important correlation with the reported anthropogenic emissions, one should be cautious when extrapolating it to global acceleration. Raupach et al. (2007) suggested that 54% of the global increase in CO₂ emissions from fossil

fuel combustion and cement manufacturing over the 2001–2006 periods came from China alone. Gregg et al. (2008) demonstrated that China became the largest national source of CO₂ emissions during recent years. Consequently, the much faster increase rates even in remote western China would certainly play a huge role in global emissions. Additionally, the rising respiration in autumn due to climate change and autumn warming (Piao et al., 2008) may happen. However, we assume the contribution to the overall trend should be much less compared to the fossil fuels and other human sources.

3.2.5. Trends of CO₂ sinks. Although no apparent upward or downward trend was observed during the 1995–2008 period for the overall change of CO₂ sinks, two peaks were present in 2005 and 2007 (Fig. 9). Mean ΔCO_2 (W_S) varied from $-86.0 \text{ Tg C yr}^{-1}$ in 1995–1999 to $-106.2 \text{ Tg C yr}^{-1}$ in 2005–2008. This may yet imply an increasing trend of CO₂ sinks in the region. Because the trend was only observed in summer (Fig. 8), we infer that it is attributed to enhanced CO₂ fluxes of vegetation absorption.

Several studies have reported increasing trends of carbon sinks in China driven by land-use changes or climate change based on both observations of inventory as well as satellite data and model simulations (Fang et al., 2001, 2004; Lal, 2004; Huang and Sun, 2006; Piao et al., 2007, 2009). For example, Fang et al. (2004) found that the increased summer precipitation in China may have benefited vegetation growth as the large-scale reforestation and afforestation programs conducted since the 1980s have been confirmed by Fang et al. (2001) as being the main causes of regional carbon sinks.

Precipitation has increased significantly in western China during the past 50 yr (Zhai et al., 2005). The changes in precipitation amount and distribution would alter current regional and global-scale terrestrial carbon cycles. This is likely associated with enhanced CO₂ sinks in western regions of China by our estimation and in addition, changes in land cover/use (e.g. the strategy of returning the grain plots to forestry and grass) over past decades may be another factor that increases carbon sinks in the region (Tian et al., 2011a).

However, the growth rate of CO₂ sinks cannot keep up with the increase in CO₂ emissions in the region which results in the continuous increase of atmospheric loading of CO₂ mixing ratios that will greatly impact the global carbon cycle. According to past records, the atmospheric temperature measured at Waliguan increased by more than 0.6°C/decade, which is much faster than the global land mean temperature growth rates of $\sim 0.27^\circ\text{C}/\text{decade}$ (IPCC, 2007). The rapid growth rate of atmospheric temperature

implies that the region is sensitive to climate change. Therefore, further studies including more regional data with high spatial resolutions and more developed models like the atmospheric inverse model and process-based ecosystem models are needed in order to illustrate our results.

4. Conclusions

We have implied changes in CO₂ emissions and sinks in western China over the 1995–2008 period based on the long-term dataset of atmospheric CO₂ at Waliguan. Changes in CO₂ emissions and sinks are estimated from episodes of elevated and sequestered CO₂ concentrations selected by a modified background identification method. With this method, we have identified nearly $17.2\% \pm 1.2\%$ and $10.1\% \pm 0.8\%$ of all observed data as elevated and sequestered CO₂, respectively. We propose that the CO₂ emissions of western China have increased significantly in all seasons during the past 14 yr, with a growth rate of $\sim 8.4 \text{ Tg C yr}^{-1}$ ($3.9\% \text{ yr}^{-1}$) during 1995–2008. We estimate the growth trend has steadily increased $12.6 \text{ Tg C yr}^{-1}$ ($6.2\% \text{ yr}^{-1}$) since 2000.

The growth rates of CO₂ emissions from western China are lower than that estimated from all of China by Gregg et al. (2008), but higher than the simulations for the global CO₂ emission trend by Le Quere et al. (2009) on the basis of the national energy statistics and by Raupach et al. (2007) during the same periods. We also find that CO₂ sinks in western China varied from $86.0 \text{ Tg C yr}^{-1}$ in early 1995–1999 to $106.2 \text{ Tg C yr}^{-1}$ in recent 2005–2008.

According to the seasonal changes of CO₂ sinks, we have demonstrated that the change is closely related to the summer enhancement of CO₂ sequestration by the vegetation photosynthesis effect during the growing season in the Northern hemisphere. Thus, we suppose the increase of CO₂ sinks may be related to increased precipitation and changes in land use over past decades in western China. The growth rate of CO₂ sinks cannot keep up with the increase of CO₂ emissions in the region, which will result in a continuous increase of atmospheric CO₂ mixing ratios and finally influence global CO₂ loadings in the future.

Although this relatively comprehensive analysis is intended to identify the changes of CO₂ emissions and sinks in the west area of China, it is also critical to recognize the limitation of the current method. Because of the complicated sources and sinks of CO₂ in terrestrial systems in China, it is necessary to use more regional input data with higher temporal and spatial resolutions for carbon fluxes estimation in the future. Furthermore, we will apply other models like the atmospheric inverse and process-based ecosystem models to simulate and derive more confident estimations.

5. Acknowledgements

This work was supported by the National Natural Science Foundation of China (41175116), National Basic Research Program of China '973' (Grant No. 2010CB950601, 2013CB955801) and International S&T Cooperation Program of MOST (Grant No. 2011DFA21090). Data used are supplied by the Chinese Academy of Meteorological Sciences (CAMS), China Meteorological Administration (CMA). The paper is based on F. Zhang's PhD program from 2008–2011 during her study in CAMS. We thank the staff of Waliguan Station for their efforts in maintain in-situ measurement systems. We also appreciate two anonymous reviewers for their constructive comments that greatly improved this manuscript. Finally, we would like to thank Mr. Timothy Logan's assistance in correcting the English.

References

- Bai, W. G., Zhang, X. Y. and Zhang, P. 2010. Temporal and spatial distribution of tropospheric CO₂ over China based on satellite observations. *Chin. Sci. Bull.* **55**(31), 3612–3618.
- Ballantyne, A. P., Alden, C. B., Miller, J. B., Tans, P. P. and White, J. W. C. 2012. Increase in observed net carbon dioxide uptake by land and oceans during the past 50 years. *Nature*. **488**. DOI: 10.1038/nature11299.
- Bousquet, P., Peylin, P., Ciais, P., Le Quere, C., Friedlingstein, P. and co-authors. 2000. Regional changes in carbon dioxide fluxes of land and oceans since 1980. *Science*. **290**, 1342–1346.
- Bousquet, P., Peylin, P., Ciais, P., Ramonet, M. and Monfray, P. 1999. Inverse modelling of annual atmospheric CO₂ sources and sinks 2. Sensitivity study. *J. Geophys. Res.* **104**(D21), 26179–26193.
- Canadell, J. G., Le Quere, C., Raupach, M. R., Field, C. B., Buitenhuis, E. T. and co-authors. 2007. Contributions to accelerating atmospheric CO₂ growth from economic activity, carbon intensity, and efficiency of natural sinks. *Proc. Natl. Acad. Sci. U. S. A.* **104**, 18866–18870.
- Draxler, R. R. and Hess, G. D. 1998. An overview of the HYSPLIT 4 modelling system for trajectories, dispersion, and deposition. *Aust. Meteorol. Mag.* **47**, 295–308.
- Fan, S., Gloor, M., Mahlman, J., Pacala, S., Sarmiento, J. and co-authors. 1998. A large terrestrial carbon sink in North America implied by atmospheric and oceanic carbon dioxide data and models. *Science*. **282**, 442–446.
- Fang, J. Y., Chen, A. P., Peng, C. H., Zhao, S. Q. and Ci, L. J. 2001. Changes in forest biomass carbon storage in China between 1949 and 1998. *Science*. **292**, 2320–2322.
- Fang, J. Y., Piao, S. L., He, J. S. and Ma, W. H. 2004. Increasing terrestrial vegetation activity in China, 1982–1999. *Sci. China. C. Life. Sci.* **47**, 229–240.
- Francey, R. J., Tans, P. P., Allison, C. E., Enting, I. G., White, J. W. C. and co-authors. 1995. Changes in oceanic and terrestrial carbon uptake since 1982. *Nature*. **373**, 326–330.
- Francey, R. J., Trudinger, C. M., Schoot, M. V. D., Krummel, P. B., Steele, L. P. and co-authors. 2010. Differences between trends in atmospheric CO₂ and reported trends in anthropogenic CO₂ emissions. *Tellus. B.* **62**, 316–328.
- Gillette, D. A., Komhyr, W. D., Waterman, L. S., Steele, L. P. and Gammon, R. H. 1987. The NOAA/GMCC continuous CO₂ record at the South Pole, 1975–1982. *J. Geophys. Res.* **92**, 4231–4240.
- Gregg, J. S., Andres, R. J. and Marland, G. 2008. China: emissions pattern of the world leader in CO₂ emissions from fossil fuel consumption and cement production. *Geophys. Res. Lett.* **35**, L08806. DOI: 10.1029/2007GL032887.
- Guan, D., Liu, Z., Geng, Y., Lindner, S. and Hubacek, K. 2012. The gigatonne gap in China's carbon dioxide inventories. *Nat. Clim. Chang.* **2**, 672–675.
- Gurney, K. R., Law, R. M., Denning, A. S., Rayner, P. J., Baker, D. and co-authors. 2002. Towards robust regional estimates of CO₂ sources and sinks using atmospheric transport models. *Nature*. **415**, 626–630.
- House, J. I., Prentice, C., Ramankutty, N., Houghton, R. A. and Heimann, M. 2003. Reconciling apparent inconsistencies in estimates of terrestrial CO₂ sources and sinks. *Tellus B.* **55B**, 345–363.
- Huang, Y. and Sun, W. J. 2006. Changes in topsoil organic carbon of croplands in mainland China over the last two decades. *Chin. Sci. Bull.* **51**(15), 1785–1803.
- IPCC. 2007. *Climate Change 2007: The Physical Science Basis*. Cambridge University Press, Cambridge.
- Khélifa, N., Lecollinet, M. and Himbert, M. 2007. Molar mass of dry air in mass metrology. *Measurement*. **40**, 779–784.
- Lal, R. 2004. Offsetting China's CO₂ emissions by soil carbon sequestration. *Clim. Chang.* **65**, 263–275.
- Le Quere, C., Raupach, M. R., Canadell, J. G., Marland, G., Bopp, L. and co-authors. 2009. Trends in the sources and sinks of carbon dioxide. *Nat. Geosci.* **2**, 831–836.
- Liu, L. X., Zhou, L. X., Zhang, X. C., Wen, M., Zhang, F. and co-authors. 2009. The characteristics of atmospheric CO₂ concentration variation of four national background stations in China. *Sci. China. Ser. D. Earth. Sci.* **52**(11), 1857–1863.
- Lu, C., Tian, H. Q., Liu, M., Ren, W., Xu, X. and co-authors. 2012. Effects of nitrogen deposition on China's terrestrial carbon uptake in the context of multiple environmental changes. *Ecol. Appl.* **22**, 53–75.
- Maksyutov, S., Machida, T., Mukai, H., Patra, P. K., Nakazawa, T. and co-authors. 2003. Effect of recent observations on Asian CO₂ flux estimates by transport model inversions. *Tellus. B.* **55**, 522–529.
- Mu, Q. Z., Zhao, M. S., Running, S.W., Liu, M. L. and Tian, H. Q. 2008. Contribution of increasing CO₂ and climate change to the carbon cycle in China's ecosystems. *J. Geophys. Res.* **113**, G01018. DOI: 10.1029/2006JG000316.
- Pacala, S. W., Hurtt, G. C., Baker, D., Peylin, P., Houghton, R. A. and co-authors. 2001. Consistent land- and atmosphere-based U.S. carbon sink estimates. *Science*. **292**, 2316–2320.
- Peters, G. P., Marland, G., Le Quéré, C., Boden, T., Canadell, J. G. and co-authors. 2012. Rapid growth in CO₂ emissions

- after the 2008–2009 global financial crisis. *Nat. Clim. Chang.* **2**, 2–4.
- Peylin, P., Bousquet, P., Le Quéré, C., Sitch, S., Friedlingstein, P. and co-authors. 2005. Multiple constraints on regional CO₂ flux variations over land and oceans. *Glob. Biogeochem. Cycles*. **19**(1), 2214–2237.
- Piao, S. L., Ciais, P., Friedlingstein, P., Peylin, P., Reichstein, M. and co-authors. 2008. Net carbon dioxide losses of northern ecosystems in response to autumn warming. *Nature*. **451**, 49–52.
- Piao, S. L., Fang, J. Y., Ciais, P., Peylin, P., Huang, Y. and co-authors. 2009. The carbon balance of terrestrial ecosystems in China. *Nature*. **458**, 1009–1013.
- Piao, S. L., Fang, J. Y., Zhou, L. M., Tan, K. and Tao, S. 2007. Changes in biomass carbon stocks in China's grasslands between 1982 and 1999. *Glob. Biogeochem. Cycles*. **21**, GB2002. DOI: 10.1029/2005GB002634.
- Raupach, M., Marland, G., Ciais, P., L Quéré, C., Canadell, J. G. and co-authors. 2007. Global and regional drivers of accelerating CO₂ emissions. *Proc. Natl. Acad. Sci.* **104**, 10288–10293.
- Ren, W., Tian, H. Q., Tao, B., Huang, Y. and Pan, S. 2012. China's crop productivity and soil carbon storage as influenced by multifactor global change. *Glob. Chang. Biol.* **18**, 2945–2957.
- Ren, W., Tian, H. Q., Xu, X., Liu, M., Lu, C. and co-authors. 2010. Spatial and temporal patterns of CO₂ and CH₄ fluxes in China's croplands in response to multifactor environmental changes. *Tellus. B.* **63B**, 222–240.
- Rousseau, D. D., Duzer, D., Etienne, J. L., Cambon, G., Jolly, D. and co-authors. 2004. Pollen record of rapidly changing air trajectories to the North Pole. *J. Geophys. Res.* **109**, D06116. DOI: 10.1029/2003JD003985.
- Sarmiento, J. L., Gloor, M., Gruber, N., Beaulieu, C., Jacobson, A. R. and co-authors. 2010. Trends and regional distributions of land and ocean carbon sinks. *Biogeosciences*. **7**, 2351–2367.
- Stohl, A. 1996. Trajectory statistics – a new method to establish source-receptor relationships of air pollutants and its application to the transport of particulate sulfate in Europe. *Atmos. Environ.* **30**, 579–587.
- Tans, P. P., Bakwin, P. S. and Guenther, D. W. 1996. A feasible global carbon cycle observing system: a plan to decipher today's carbon cycle based on observations. *Glob. Chang. Biol.* **2**, 309–318.
- Tans, P. P., Fung, I. Y. and Takahashi, T. 1990. Observational constraints on the global atmospheric CO₂ budget. *Science*. **247**, 1431–1438.
- Tian, H. Q., Melillo, J., Lu, C., Kicklighter, D., Liu, M. and co-authors. 2011a. China's terrestrial carbon balance: contribution from multiple global change factors. *Glob. Biogeochem. Cycles*. **25**. DOI: 10.1029/2010GB003838.
- Tian, H. Q., Xu, X., Lu, C., Liu, M., Ren, W. and co-authors. 2011b. Net exchanges of CO₂, CH₄, and N₂O between China's terrestrial ecosystems and the atmosphere and their contributions to global climate warming. *J. Geophys. Res.* **116**, 1393–1405.
- Trenberth, K. E. and Smith, L. 2005. The mass of the atmosphere: a constraint on global analyses. *J. Clim.* **18**, 864–875.
- Thoning, K., Tans, P. P. and Komhyr, W. 1989. Atmospheric carbon dioxide at Mauna Loa Observatory, 2. Analysis of the NOAA GMCC data, 1984–1985. *J. Geophys. Res.* **94**, 8549–8565.
- Turnbull, J. C., Tans, P. P., Lehman, S. J., Baker, D., Conway, T. J. and co-authors. 2011. Atmospheric observations of carbon monoxide and fossil fuel CO₂ emissions from East Asia. *J. Geophys. Res.* **116**, D24306. DOI: 10.1029/2011JD016691.
- Wang, G. C., Wen, Y. P. and Kong, Q. X. 2002. The concentration of CO₂ and its variation in China. *Chin. Sci. Bull.* **47**(10), 780–783.
- Wang, Y., Munger, J. W., Xu, S., McElroy, M. B., Hao, J. and co-authors. 2010. CO₂ and its correlation with CO at a rural site near Beijing: implications for combustion efficiency in China. *Atmos. Chem. Phys.* **10**(18), 8881–8897.
- Wen, Y. P., Tang, J., Shao, Z. Q., Zhang, X. C. and Zhao, Y. C. 1997. A study of atmospheric CO₂ concentration variations and emission from the soil surface at MT. Waliguan. *Q. J. Appl. Meteorol.* **8**, 129–136.
- Zhai, P., Zhang, X., Wan, H. and Pan, X. 2005. Trends in total precipitation and frequency of daily precipitation extremes over China. *J. Clim.* **18**, 1096–1108.
- Zhang, D. Q., Tang, J., Shi, G. Y., Nakazawa, T., Aoki, S. and co-authors. 2008. Temporal and spatial variations of the atmospheric CO₂ concentration in China. *Geophys. Res. Lett.* **35**(3), L03801. DOI: 10.1029/2007GL032531.
- Zhang, F., Zhou, L. X., Novelli, P. C., Worthy, D. E. J., Zellweger, C. and co-authors. 2011. Evaluation of in situ measurements of atmospheric carbon monoxide at Mount Waliguan, China. *Atmos. Chem. Phys.* **11**(11), 5195–5206.
- Zhou, L. X., Conway, T. J., White, J. W. C., Mukai, H., Zhang, X. and co-authors. 2005. Long-term record of atmospheric CO₂ and stable isotopic ratios at Waliguan Observatory: background features and possible drivers, 1991–2002. *Glob. Biogeochem. Cycles*. **19**, GB3021. DOI: 10.1029/2004GB002430.
- Zhou, L. X., Tang, J., Wen, Y. P., Li, J. L. and Yan, P. 2003. The impact of local winds and long-range transport on the continuous carbon dioxide record at Mount Waliguan, China. *Tellus. B.* **55**, 145–158.
- Zhou, L. X., White, J. W. C., Conway, T. J., Mukai, H., MacClune, K. and co-authors. 2006. Long-term record of atmospheric CO₂ and stable isotopic ratios at Waliguan Observatory: seasonally averaged 1991–2002 source/sink signals, and a comparison of 1998–2002 record to the 11 selected sites in the Northern Hemisphere. *Glob. Biogeochem. Cycles*. **20**, GB2001. DOI: 10.1029/2004GB002431.